Available online at www.sciencedirect.com
SCIENCE DIRECT
Polymer 47 (2006) 3372–3381
polymer
www.elsevier.com/locate/polymer

Adsorption of bovine serum albumin and fibrinogen on hydrophilicity-controllable surfaces of polypyrrole doped with dodecyl benzene sulfonate—A combined piezoelectric quartz crystal impedance and electrochemical impedance study

Meiling Liu [a], Youyu Zhang [a,b,*], Meiling Wang [a], Chunyan Deng [a], Qingji Xie [a], Shouzhuo Yao [a,b]

[a] *Key Laboratory of Chemical Biology and Traditional Chinese Medicine Research (Ministry of Education, China), College of Chemistry and Chemical Engineering, Hunan Normal University, Changsha 410081, People's Republic China*
[b] *College of Chemistry and Chemical Engineering, Hunan University, Changsha 410082, People's Republic China*

Received 28 June 2005; received in revised form 18 January 2006; accepted 5 March 2006
Available online 3 April 2006

Abstract

Combined measurements of piezoelectric quartz crystal impedance (PQCI) and electrochemical impedance (EI) were utilized to monitor in situ adsorption of two proteins (bovine serum albumin and fibrinogen) onto the hydrophilicity-controllable surfaces of polypyrrole (PPY) doped with dodecyl benzene sulfonate (DBS). Three of these polymer films, PPY/DBS-I, PPY/DBS-II and PPY/DBS-III, were obtained by galvanostatic electropolymerization of pyrrole in aqueous solutions containing 0.6, 1.2 and 2.0 mmol L^{-1} sodium dodecyl benzene sulfonate (SDBS), respectively. The PPY/DBS-II obtained from electropolymerization of pyrrole in the presence of 1.2 mmol L^{-1} SDBS (the critical micelle concentration of SDBS in aqueous solution, CMC) exhibited the greatest hydrophobicity, as suggested by contact angle measurement. And the saturation-adsorption amounts for both proteins were found to be greatest on the surface. The kinetics and adsorption mechanisms of both proteins adsorbed on these three surfaces were discussed. Langmuir and Freundlich models were used for explaining the adsorption behavior of proteins, giving that Langmuir model is better for bovine serum albumin (BSA) and both model are not so available for fibrinogen.

Keywords: Piezoelectric quartz crystal impedance (PQCI); Electrochemical impedance spectroscopy (EIS); Polypyrrole doped with dodecyl benzene sulfonate (SDBS)

1. Introduction

The interaction of proteins with solid surfaces is not only a fundamental phenomenon but also a key to several important and novel applications in biosensors, medical devices and biotechnology [1–3]. In biomaterial field, protein adsorption is the first process in integration of an implanted material or device into tissue [4,5]. For example, the adsorption of serum proteins, such as fibronectin and fibrinogen can influence the adhesion of macrophages or platelets, and ultimately leads to fibrous encapsulation [6,7]. In biotechnology field, protein/surface interactions are crucial for assembly of interfacial protein construction. Therefore, detailed mechanism understanding of protein/surface interaction would be of great value to all of these fields, and the ability to trace specific protein/surface interactions will benefit the nanoscale materials and bio-nano-assembly technology [8]. There are two primary methods to study the protein adsorption on solid surface: fabricating selective templates [9,10] or adopting self-assembly monolayer (SAM) [11] for protein adsorption. Therefore, studying the bonding of proteins with these templates or SAM may increase our knowledge of protein biophysics in general.

Many techniques, including fluorescence [1], FT-IR [12], UV–VIS [13], scanning electron microscope (SEM) [1,14], radiolabelling [1], surface plasma resonance (SPR) [15], piezoelectric quartz crystal (PQC) sensor [16] and electrochemical impedance spectroscopy (EIS) [17,18], have been used to investigate surface adsorption of biological substances or other species. Among them, SPR, PQC and EIS are able to investigate surface adsorption both in situ and ex situ.

* Corresponding author. Address: Chemical Research Institute, Hunan Normal University, Lushan Road 36, Changsha, Hunan 410081, People's Republic China. Tel./fax: +86 731 8865515.
E-mail address: zhangyy@hunnu.edu.cn (Y. Zhang).

0032-3861/$ - see front matter © 2006 Elsevier Ltd. All rights reserved.
doi:10.1016/j.polymer.2006.03.019

Piezoelectric quartz crystal impedance (PQCI) method can provide multidimensional piezoelectric information and characterize the PQC resonance completely [19–24]. The Sauerbrey equation describing a frequency–mass relationship for loading or removal of a rigid and thin film [19] is given as follows:

$$\Delta f_0 = -2f_{0g}^2 \frac{\Delta m}{A\sqrt{\rho_q \mu_q}} = -2.264 \times 10^{-6} f_{0g}^2 \frac{\Delta m}{A} \quad (1)$$

where Δf_0 is the measured frequency shift (Hz), f_{0g} is the parent frequency of QCM (9×10^6 Hz), Δm is the adsorption amount (ng), ρ_Q is the density of quartz (2.65 g cm^{-3}), μ_Q is the shear modulus of quartz (2.947×10^{10} dyn m^{-2}), and A is the effective area of the electrode (0.29 cm^2). Replacing f_{0g}, ρ_Q, μ_Q and A in Eq. (1) with the above actual values for 9 MHz PQC yields Eq. (2):

$$\Delta f_0 = (2.1 \pm 0.1)\Delta m \quad (2)$$

In addition, it is known that Eq. (1) can be used for the solution system under specific conditions where the influence of the visco-elasticity of the polymer is negligible [19,25]. A net liquid-loading effect for a PQC with one side contacting solution can be characterized by the following equation [21,22]:

$$2\pi L_{1q}\delta\Delta f_{G1/2L} \approx \Delta R_{1L} = 2\pi f \Delta L_{1L}$$

$$= -4\pi L_{1q}\Delta f_{0L}\sqrt{f\mu_q}/\sqrt{f_{0g}\bar{c}_{66}} \approx -4\pi L_{1q}\Delta f_{0L} \quad (3)$$

where $\delta\Delta f_{G1/2L}$, Δf_{0L}, ΔR_{1L} and ΔL_{1L} are changes in $\Delta f_{G1/2}$ (the half peak width of the conductance curve), f_{0L} (the resonant frequency, and $f_{0L} = 1/[2\pi(L_1C_1)^{1/2}]$), R_1 and L_1 due to the variations of solution density and viscosity, respectively. f_{0g} is the resonant frequency in air, L_{1q} is the motional inductance for the PQC in air, and $\bar{c}_{66}$ (2.957×10^{10} N m^{-2}) is the lossy piezoelectrically stiffened quartz elastic constant. According to this equation, the characteristic slope value of $\Delta f_0/\Delta R_{1L}$ for a net density/viscosity effect on the 9 MHz PQC resonance is ~ -10 Hz Ω^{-1}. Obviously, for an investigated system, the larger the absolute value of $\Delta f_0/\Delta R_{1L}$, the weaker the viscous effect and the stronger the mass effect.

Electrochemical impedance (EI) is a powerful method for investigating electrode process and determining surface adsorption kinetics as well as mass-transport parameters, through adopting smaller electrochemical perturbations [26]. The electrochemical complex impedance (Z) can be represented as a sum of a real (Z_{re}) and an imaginary (Z_{im}) component ($Z = Z_{re} + jZ_{im}$) that originate generally from the resistance and capacitance of electrolytic cell, respectively.

Owing to the complexity of protein adsorption, more information acquired in real-time is obviously helpful for intensive understanding of the biological phenomena. A combination of PQC and electrochemical impedance spectrum (EIS), namely, EQCIS, is expected to provide sufficient information of interfacial characteristics, including electrode mass, local density/viscosity near the electrode and the interfacial capacitance, etc.

Surface modification plays a key role in the development of biosensors. Organic polymers, in particular conductive polymers, have recently attracted much attention for use as supports for immobilization of proteins [27–29]. Vladyslav Kholodovych et al. presented simi-empirical models for predicting cellular response to the surface of biodegradable polymer [30] and predicting fibrinogen adsorption to polymeric surfaces in silico [31], which were important for rational design of polymeric materials in biomedical application. And Katarzyna Kita-Tokarczyk et al. presented a review of recent literature concerning amphiphilic block copolymer vesicles [32], which have recently emerged as a special class of materials. Therefore, the study of protein adsorption on polymer surface is also important for conducting biosensor. Recently, Zhang et al. [33] had reported the adsorption of BSA and fibrinogen onto different anion doped polyaniline-modified electrodes and found that the adsorption behavior of protein on polymer surface was affected by its hydrophilic/ hydrophobic and electriferous property of the polymer.

Among the investigated systems, polypyrrole (PPY) has proved to be an important conductive polymer because of its unique properties: (1) it has many advantages including environmental stability, good redox properties and high electrical conductivities [34–36], and the pyrrole monomer is easily oxidized in aqueous solutions and compatible with many biological elements; (2) PPY can be easily obtained via chemical or electrochemical methods and doped with variable anions in the films [37–39]. Sodium dodecyl benzene sulfonate (SDBS) is an anion surfactant with long carbon chain, which can be doped into PPY film and hence affects the hydrophilic property of the surface; (3) as a kind of amphiphilic substance, protein exhibits a tendency to adsorb onto both hydrophilic and hydrophobic surfaces and a considerable protein adsorption may change the electroactivity of the electrode. Consequently, studying the effect of the hydrophilicity of PPY/DBS modified surfaces on protein adsorption may be helpful for developing polymer–electrode-based electrochemical detection/sensors in vitro or in vivo.

In this paper, the hydrophilicity-controllable surfaces of polypyrrole doped with dodecyl benzene sulfonate were prepared for the first time. The hydrophilicity of the surfaces can be controlled by doping different amount of DBS. BSA and fibrinogen as model proteins were used and the adsorption processes of them were investigated by EQCIS system. According to the EQCIS measurement, the adsorption kinetics, the adsorption models and adsorption mechanisms of both proteins were investigated.

2. Experimental section

2.1. Instrumentation and chemicals

The EQCIS system used in this paper was described by Xie et al. [22], which allowed fast and simultaneous measurements of the PQC electroacoustic admittance via a HP4395A impedance analyzer and the electrochemical impedance via a CHI660A electrochemical workstation

(CH Instrument Co., USA). A suitable isolation-capacitance (C_i = 810 pF) was used to minimize the instrumentation interference on EIS measurements with CHI660A from simultaneous measurements of the PQCI with HP4395A [22]. Synchronous G and B measurements controlled by a user-written Visual Basic (VB) 5.0 program were conducted under conditions of 201 points, a frequency span of 40 kHz covering the PQC resonant frequency. Real-time acquisitions of equivalent circuit parameters at a time interval of about 1 s were also achieved with the VB 5.0 program through fitting each group of G and B data to a modified BVD model [22] based on a Gauss–Newton non-linear least-square fitting algorithm and a selection of R_1, C_0, f_0 and $1/C_1$ as estimation parameters. AT-cut 9 MHz piezoelectric quartz crystals (12.5 mm in diameter) were used experimentally. A glassy three-electrode electrolytic cell of 50 mL volume was used in this experiment. The gold electrode with a diameter of 6.5 mm on one side of the PQC contacted the solution and served as working electrode (WE), while the Ag electrode on the other side of the PQC was located in the air. The reference electrode was a saturated calomel electrode (SCE) and a carbon rode electrode was used as a counter electrode. All the potentials reported in this paper are relative to this reference electrode. Contact angles of water droplets at the given polymer-surface were measured using a JJC-II contact-angle measurement instrument (Changchun Fifth Optical Instruments Factory, China). Scanning electron microscope (SEM) photographs were taken on a Hitachi S-570 SEM. Fourier transform infrared (FT-IR) spectra were collected on a Nicolet Nexus 670 FT-IR instrument (Nicolet Instrument Co., Madison, WI) with transmission mode. Experimental operations are depicted as follows. A piece of transparent minigrid electrode of stainless steel in $1.8 \times 2.4\ cm^2$ size was coated with a thin-layer gold through sputtering from a gold target of 99.99% purity for 40 min under the pressure of 7 mmHg and 2 mA current (Zhongkekeyi SBC-12 ion coater, Beijing). The details of minigrid specification are as follows, diameter of metal wire = 25 μm, size of metal wires-enclosed rectangular hole = 30 × 30 μm, and both holes and wires are uniformly distributed, as examined by an optical microscope (Olympus CH30, Japan). The prepared Au minigrid electrode was used as WE during polymerization, which was partially immersed in the polymerization solution. After polymerization, the obtained polymer-modified Au minigrid electrode was thoroughly washed and dried, and then subjected to FT-IR measurements in the transmission mode. All FT-IR spectra were acquired with a wave number resolution of $4\ cm^{-1}$ and an average factor of 100. The parts of bare Au minigrid that was not immersed in the polymerization bath were used as the Ref. [40].

Pyrrole, BSA (molecular weight, M_w, 67,000) and fibrinogen (M_w 340,000) were purchased from Sigma. And pyrrole was distilled prior to use. Phosphate buffer solution (PBS, pH = 7.0) was made up of NaH_2PO_4 and K_2HPO_4. The stock protein solution was prepared by adding the protein into $0.1\ mol\ L^{-1}$ PBS and stored at 4 °C before use. NaAc–HAc buffer solution (pH = 5.1) was prepared by mixing $0.1\ mol\ L^{-1}$ HAc and $0.2\ mol\ L^{-1}$ NaAc together. All other chemicals were analytical grade or better. Doubly distilled water and freshly prepared solutions were used throughout. All experiments were carried out at room temperature.

2.2. Procedures

2.2.1. Preparation of PPY/DBS-modified electrode

To remove surface oxides or possible surface contamination, the gold plate electrode and the PQC electrode were first treated with nitric acid, and then cyclic scanned between 0 and 1.5 V versus SCE in $0.2\ mol\ L^{-1}$ $HClO_4$ aqueous solution till reproducible cyclic voltammograms were obtained [41]. PPY/DBS films were prepared by galvanostatic electropolymerization of pyrrole at constant current of 12 or 10 μA in $10\ mmol\ L^{-1}$ pyrrole aqueous solution containing different concentrations of SDBS. When the frequency of the PQC electrode decreased by about 5200 Hz in solution, the polymerization was manually stopped. To obtain stable films for protein adsorption and eliminate the effect of different open-circuit relaxation time, the electrodes were placed in the solution for 2 min after polymerization [42].

2.2.2. Characterization of the PPY/DBS-modified electrode

The hydrophilic/hydrophobic properties of electropolymerized PPY/DBS films were first characterized by contact angle experiment. Contact angles of water droplets at the electrodeposited polymer surfaces were measured after the PPY/DBS films were obtained. Then, the surfaces of the polymer-modified electrode were observed with scanning electron microscope (SEM). According to the results of the contact angles and SEM photographs, three representative polymer films, PPY/DBS-I, PPY/DBS-II and PPY/DBS-III obtained from electropolymerization in $10\ mmol\ L^{-1}$ pyrrole solutions in the presence of 0.6, 1.2 and $2.0\ mmol\ L^{-1}$ SDBS, respectively, were chosen for further research.

2.2.3. Adsorption of protein onto PPY/DBS-modified electrode surfaces

BSA and fibrinogen adsorbed onto the newly prepared and representative PPY/DBS modified PQC electrodes (PPY/DBS-I, PPY/DBS-II and PPY/DBS-III) were conducted in $0.1\ mol\ L^{-1}$ PBS (pH = 7.0) in the absence of electroactive species under magnetic stirring. The stock protein solution was firstly added into PBS when stable frequency of the PQC electrode was obtained and then added at every 250 s (for BSA) or 300 s (for fibrinogen) till there was no obvious change in the frequency. PQCI and EIS were conducted simultaneously during the process. The saturated adsorption concentrations of both proteins on the three surfaces could be calculated. For studying the protein adsorption kinetics and adsorption models, the maximum saturated adsorption concentrations of both proteins were used.

3. Results and discussion

3.1. Preparation and characterization of PPY/DBS films

Three electropolymerization techniques, potentiostatic, galvanostatic and potential sweep had been used to prepare PPY film. In this work, galvanostatic electropolymerization was chosen for preparation of the PPY/DBS-modified electrode because it is easier for utilizing this method to describe the film quantitatively and investigating the macroscopic film growth [42]. In order to avoid overoxidation of pyrrole, the current was fixed at 12 μA or lower during the film growth. Thus under this experimental condition, the potential can be controlled slightly lower than 0.8 V and pyrrole can be prevented from overoxidation. At the oxidative potential, pyrrole radical cations were easily generated and then coupled to form oligmers. The oligmers eventually deposited together with the doped anions on the gold electrode. Fig. 1 shows the piezoelectric quartz crystal impedance response during the preparation of PPY/DBS-I, PPY/DBS-II and PPY/DBS-III. According to our previous research, the effect of the thickness of the films could be neglected [33] and therefore arbitrary thickness can be used to investigate protein adsorption behavior on the polymer-modified surface. In this work, the thickness was controlled by the frequency shift of PQC (each film was manually controlled to be 5200 Hz). Fig. 1 shows that both the frequencies and the resistances decreased in all of these three electropolymerization proceedings. The $\Delta f_0/\Delta R_{1L}$ values of all the films are larger than 100, which suggested that the films were rigid and compact. Therefore, the net density/viscosity effect was weaker and could be neglected [25] and then the Sauerbrey equation (Eq. (1)) can be used to calculate the mass of the deposited films. Moreover, the difference in $\Delta f_0/\Delta R_{1L}$ values might result in difference in morphology owing to the difference in compactness of them and the absolute value of $\Delta f_{0L}/\Delta R_{1L}$ of PPY/DBS-II (187) is larger, which indicates that it is more compact than the other two (147,144). And the scanning electron microscope (SEM) photographs of these three films are shown in Fig. 2 and it can give some information of the relationship between the mechanical properties and microstructures [14]. It can be observed that the PPY/DBS-II film was more compact and homogeneous than the other two. And the PPY/DBS-III (Fig. 2(c)) is much looser which might be affected by the micelle of SDBS in the polymerization process.

For further determining the structure of the polymer and finding whether DBS doped into the films, the FT-IR spectra was collected, as shown in Fig. 3. The band of 1548 cm^{-1} is attributed to the combination stretch vibration of C–C and C=C, the band of 1458 cm^{-1} is attributed to the C–N bond stretch vibration, and the band of 1294 cm^{-1} is ascribed to the deform vibration of C–H and N–H. The 787, 670 cm^{-1} bands can be ascribed to out plane bound vibration of C–H [43]. While the bands of 1174 and 1048 cm^{-1} are attributed to the S=O stretch vibration of the character absorption of DBS [44]. Therefore, the PPY/DBS was formed under the adopted experimental conditions in this work. There are positively radicals in PPY of oxidation state and they would form complex with DBS, which is negatively charged. And the mechanism of the complex formation is shown in Scheme 1. When the concentration of DBS is lower than the critical micelle concentration (CMC), the positive radical of PPY can combine DBS easily. While with the concentration beyond CMC, the PPY positive radical can be found bonding to individual micelles, and it is more difficult to form complex [33]. Therefore, doping DBS into PPY film is difficult due

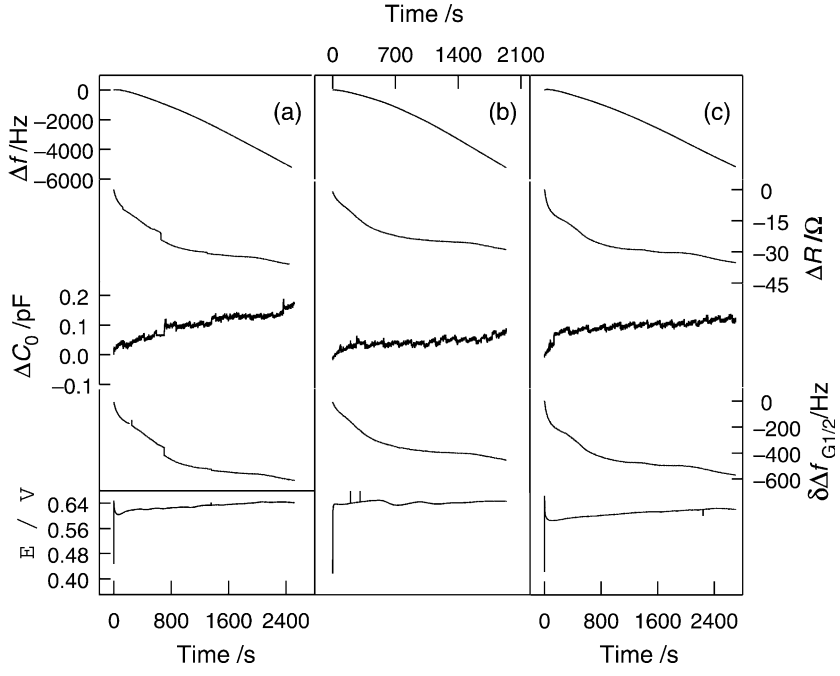

Fig. 1. Polymerization of pyrrole in 10 mmol L^{-1} pyrrole aqueous solution contained different concentrations of SDBS. (a) 0.6 mmol/L SDBS, (b) 1.2 mmol/L SDBS, (c) 2.0 mmol/L SDBS.

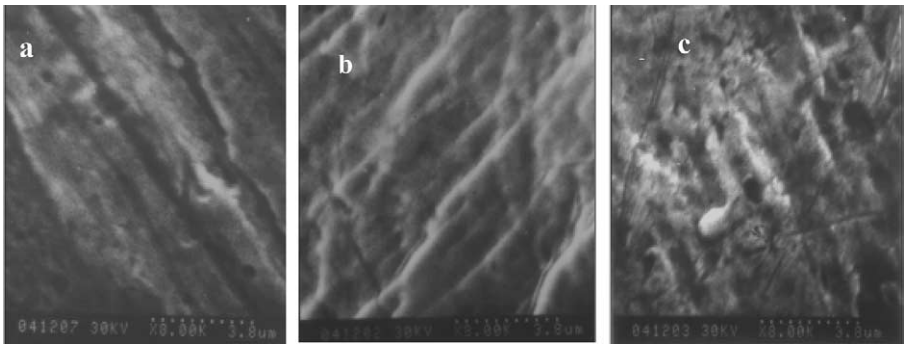

Fig. 2. The SEM photographs of PPY/SDBS films. (a) PPY/DBS-I, (b) PPY/DBS-II, (c) and PPY/DBS-III.

to the micellization of SDBS in solution, leading to fewer amounts of DBS doped into the film.

To estimate the amount of DBS in the polymer films, the interaction of brilliant cresyl blue (BCB) with DBS [45] on the electrode surfaces was monitored. Fig. 4 shows the frequency shift response of PQC resonance with time after adding BCB solution to HAc–NaAc buffer solution while stirring at a constant rate. From Fig. 4, we can see that the frequency shift was gentle when BCB was added into the buffer solution in the case of de-doped PPY film-modified electrode (the dedoped PPY film was obtained by expelling the ClO_4^- ions from PPY /ClO_4^- film electrodeposited from 10 mmol L^{-1} pyrrole in the presence of 0.2 mol L^{-1} $HClO_4$ solution) or bare gold electrode were used. The large frequency shift shown in Fig. 4 was resulted from BCB bounding to DBS on the electrode in the experiment due to the formation of DBS-BCB complex [45]. The binding molar ratio of BCB with DBS was 1:1; the amount of DBS on electrode is equally to the amount of the bound BCB. Therefore, the amount of DBS in PPY/DBS-I, PPY/DBS-II and PPY/DBS-III can be estimated according to the frequency change of PQC resonance. The dedoped PPY-modified electrode was chosen as a reference, and therefore, the frequency response caused by the net solution density and viscosity change or BCB adsorption on the PPY film was subtracted from the frequency shift in the corresponding experiments. The Δf caused by BCB binding on PPY/DBS-I, PPY/DBS-II and PPY/DBS-III were 65.0, 83.5 and 48.3 Hz and consequently, the values of DBS in three films were 9.7×10^{-11}, 1.23×10^{-10} and 7.2×10^{-11} mol, respectively.

In order to study the hydrophilic/hydrophobic properties of the films prepared at different concentrations of SDBS, the contact angles of water droplets at electrodeposited polymer surfaces were measured as shown in Table 1. The results indicated that the concentration of SDBS in the polymerization solution affected the contact angle significantly. The contact angles of water droplets increased with the increasing of SDBS concentration in the polymerization bath till the maximum contact angle was obtained as the CMC of SDBS. This phenomenon could be interpreted as follows: when SDBS concentration was lower than the CMC, the SDBS doped into

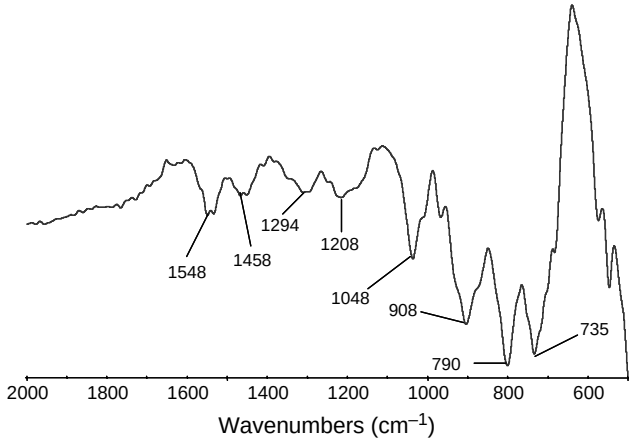

Fig. 3. The FT-IR spectra of PPY/DBS film in the transmission mode.

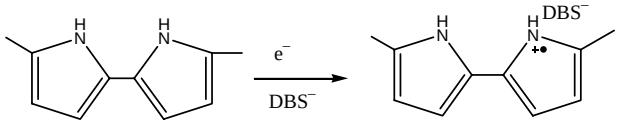

Scheme 1. The formation process of PPY/DBS.

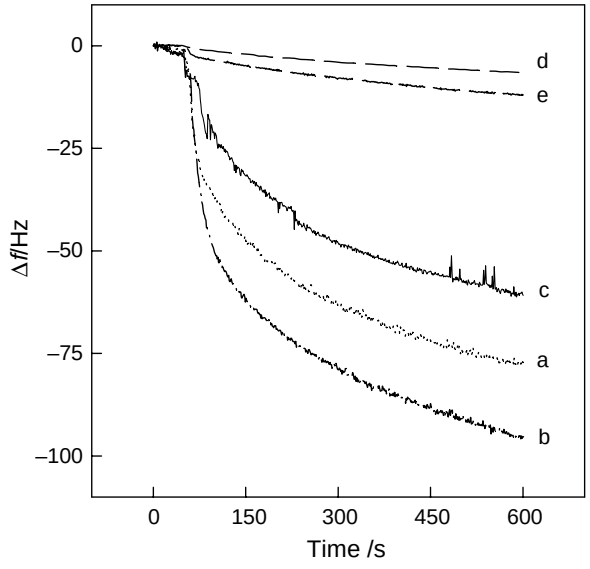

Fig. 4. The frequency responses of the (a) PPY/DBS-I, (b) PPY/DBS-II, (c) PPY/DBS-III modified electrode and (d) bare gold electrode, (e) de-doped PPY modified electrode, when adding brilliant cresyl blue in pH = 5.1 HAc–NaAc buffer solution under magnetic stirring. The final concentration of brilliant cresyl blue is 0.25 mM.

Table 1
The contact angles of the PPY/DBS films modified gold plate electrodes prepared in 10 mmol L^{-1} pyrrole aqueous solution in the presence of different concentrations of SDBS

C_{SDBS} (mmol L^{-1})	Contact angle (°)
0.45	67
0.60	76
0.90	75
1.10	79
1.20	85
1.60	77
2.00	65

Polymerization time was 2000 s and the water drops used in contact angle measurement was 20 μL.

PPY increased with its concentration increasing. While its concentration beyond the CMC, the micelle of SDBS was formed [46] and SDBS doping into PPY became more difficult. This would result in incorporation of different amount of DBS, which might affect the free energy of the PPY films by changing the hydrophobic/hydrophilic properties of PPY films, hence led to the difference in contact angle. For studying the relationship between the hydrophobic property of the surface and the adsorption amount of the protein, 0.6 mmol L^{-1} (<CMC), 1.2 mmol L^{-1} (=CMC), and 2.0 mmol L^{-1} SDBS (>CMC) were chosen as electrolyte to prepare PPY/DBS electrodes for protein adsorption, the contact angles of these three resultant electrode surfaces were 76, 85 and 65°, respectively. Thus, we can conclude that the surface of PPY/DBS-II modified electrode is of the strongest hydrophobicity.

3.2. Effect of different SDBS concentration doped PPY on protein adsorption

To obtain the adsorption pattern of BSA and fibrinogen onto the obtained electrode surfaces, the saturated adsorption concentrations of both proteins on these polymer surfaces were probed at first. Fixed volume of stock protein solution was added into 0.1 mol L^{-1} PBS (pH=7.0) at fixed time intervals until a stable frequency response was obtained. Fig. 5 shows the relationship between frequency shift and the concentration of BSA or fibrinogen. The resonance frequency of PQC decreased rapidly at the initial stage and then its decreasing speed became slower in all the cases. And the final concentrations of proteins corresponding to the stable resonance frequency reached were the saturated adsorption concentrations on the tested surface, giving the values of 9.9×10^{-6}, 2.0×10^{-5}, 8×10^{-6} mol L^{-1} for BSA and 2.5×10^{-6}, 3.8×10^{-6}, 1.6×10^{-6} mol L^{-1} for fibrinogen on PPY/DBS-I, PPY/DBS-II and PPY/DBS-III surfaces, respectively. It can also be seen that the saturated adsorption concentrations were the largest on the PPY/DBS-II surface for both proteins. Fig. 5 also exhibited the change in resonance frequency of PQC related to the adsorption of the two proteins on PPY/DBS-II film was the largest which implied that the amount of adsorbed proteins on the film was greatest. It is well known that proteins can be adsorbed onto a solid surface by electrostatic interaction, hydrophobic interaction and formation of chemical

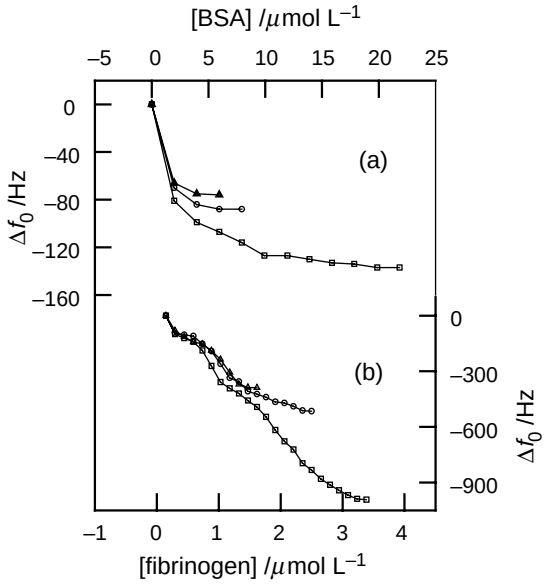

Fig. 5. The frequency responses to the concentrations of (a) BSA and (b) fibrinogen on PPY/DBS-I (circles), PPY/DBS-II (rectangles) and PPY/DBS-III (triangles) films by constantly adding stock protein solution in PBS (pH=7.0) at 250 or 300 s intervals under magnetic stirring.

bonds. The isoelectric points of BSA and fibrinogen are 4.8 and 5.3, respectively. They are both negatively charged in PBS (pH=7.0) and the polymer-modified surfaces were somewhat negatively charged due to the doped anions in the polymer. So the electrostatic interaction between the protein molecule and the polymer films could be ignored. And the formation of chemical bond between protein molecules and the tested surfaces would be impossible under this condition as well. We have mentioned above that PPY/DBS-II surface is of the strongest hydrophobicity among the three tested surfaces. Therefore, we supposed that the adsorption mainly originated from the hydrophobic interaction between the hydrophobic moiety of the protein molecules and the hydrophobic surface.

In addition, the roughness of the polymer surfaces might affect the protein adsorption. R_{ee}($R_{ee}=(\Delta f_{wet}-\Delta f_{dry})/\Delta f_{dry}$), which defined as the porosity of the prepared films, was used as the measurement for the roughness of the polymer surface and obtained by measuring the wet frequency shift ($\Delta f_{wet}=f_{0L2}-f_{0L1}$) and the dry frequency shift ($\Delta f_{dry}=f_{0g2}-f_{0g1}$) after pyrrole polymerization [47]. Before pyrrole polymerization, the stable frequency of the 9 MHz crystals in air was recorded as f_{0g1}, and the stable frequency of the 9 MHz crystals immersed in the polymerization solution was recorded as f_{0L1}. After the polymerization, the stable frequency was recorded as f_{0L2}. The electrode was then rinsed with sufficient distilled water and dried via a stream of clean air. The stable frequency in air was recorded as f_{0g2}. The results showed that R_{ee} were almost equal in all the cases, which were 13.2±2, 14.0±2 and 12.5±3% ($n=3$, n is the experiment numbers), respectively. And the resistance responses in the polymerization processes are similar as showed in Fig. 1, which also suggested that the roughness of the films are similar. Therefore,

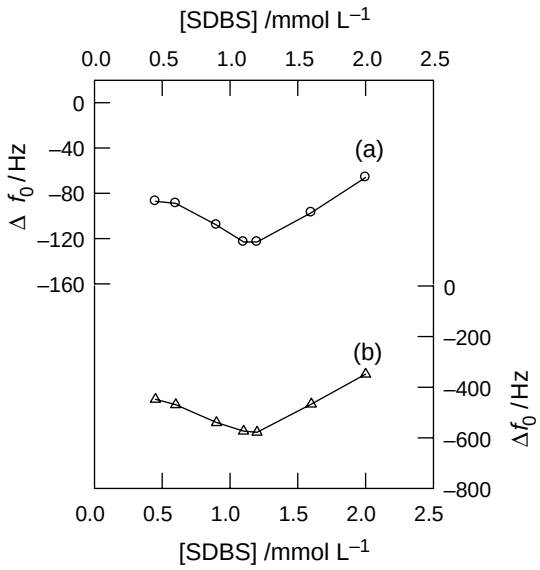

Fig. 6. The ultimately frequency change for (a) BSA or (b) fibrinogen adsorption on PPY doped with various concentration of SDBS.

the effect of the roughness on protein adsorption could be ignored as well.

To confirm the results of contact angle and the concentration of the saturated adsorption, the dependence of frequency shift on the concentration of SDBS in polymerization solution was studied. The maximum frequency shift of the protein adsorption onto different PPY/DBS modified surfaces at the saturated concentration is shown in Fig. 6. The plot indicates that the frequency shift is the largest on the electrode modified with the film prepared in the polymerization bath in the presence of 1.2 mmol L^{-1} SDBS, which consistent with the measurement results of contact angle and the measured saturated adsorption concentration. So we could conclude that 1.2 mmol L^{-1} SDBS (CMC of SDBS) doped PPY/DBS-II film modified electrode adsorbed more protein due to its more hydrophobic property.

3.3. The adsorption model of both proteins

As two model proteins, BSA and fibrinogen are usually used for studying the protein adsorption behavior on solid surface. Langmuir equation and Freundlich equation, which relate to different adsorption energy distribution patterns on the surface of the adsorbent [48,49], are used to describe the adsorption isotherms of proteins. These two equations have been used for investigating the adsorption thermodynamics of tannin adsorption on polymeric adsorbents [50]. The linear form of the Langmuir equation [48] can be expressed as:

$$\frac{1}{\Gamma_t} = \frac{1}{\Gamma_\infty} + \frac{1}{\Gamma_\infty KC} \tag{4}$$

where Γ_t is the adsorbed amount, Γ_∞ is the saturated adsorbed amount, C is the protein concentration, and K is the adsorption constant. Combining Eqs. (1) and (4), the following equation is obtained:

$$\frac{1}{\Delta f_0} = \frac{1}{\Delta f_{0,\max}} + \frac{1}{\Delta f_{0,\max} KC} \tag{5}$$

where Δf_0 is the frequency shift in Hz, $\Delta f_{0,\max}$ is the frequency shift in Hz for saturated adsorption of the protein. While the Freundlich equation can be expressed as follows [49]:

$$\Delta m = K_f C^{1/n} \tag{6}$$

where n and K_f are constants ($n > 1$), and C is the concentration of BSA or fibrinogen in the solution. Combining Eqs. (1) and (6), the following equation is obtained:

$$\Delta f_0 = K' C^{1/n} \tag{7}$$

where $K' = -2f_0 K_f/(\rho_Q \mu_Q)^{1/2} A$. For a given AT-cut quartz crystal and protein, they are all constants except Δf_0 and C. Its logarithmic form is:

$$\log \Delta f_0 = 1/n \log \Delta C + \log K' \tag{8}$$

The results obtained from fitting the experimental data in Fig. 5 to Eqs. (5) and (8) are summarized in Table 2. For all the cases of BSA adsorption, fitting the experimental data to Eq. (5), the linear regression correlation coefficients obtained are greater than 0.993, while fitting the experimental data to Eq. (8), the linear regression correlation coefficients obtained are less than 0.985. Therefore, the results indicated that the Langmuir adsorption model is more suitable to describe the adsorption behavior of BSA, and the adsorption behavior

Table 2
Fitted parameters for the Langmuir and Freundlich isotherms of two proteins

PPY (C_{SDBS}) (mmol L^{-1})	Langmuir equation			Freundlich equation		
	$\Delta f_{0,\max}$	k	r^2	k'	$1/n$	r^2
BSA						
0.6	−102	2.96×10^{11}	0.9975	2344	0.26	0.9570
1.2	−133	2.23×10^{10}	0.9965	1450	0.21	0.9836
2.0	−84	6.35×10^{11}	0.9994	444	0.13	0.9586
Fibrinogen						
0.6	−508	–	0.8206	3.94×10^{5}	0.50	0.9550
1.2	−1019	–	0.8866	6.92×10^{6}	0.69	0.9816
2.0	−473	–	0.8820	4.94×10^{5}	0.51	0.9586

$\Delta f_{0,\max}$ is the maximum frequency shift for protein adsorption; C is the equilibrium concentration of protein in solution; k and k' are adsorption equilibrium constants; $1/n$ is arbitrary constant; r^2 is correlation coefficient from linear regression.

of BSA can be described with a monolayer adsorption model. While for fibrinogen, the Langmuir and Freundlich adsorption models are not well suitable because the linear regression coefficients in all cases are less than 0.982. So the adsorption behavior of fibrinogen might not be monolayer adsorption and cannot be described by monolayer adsorption model. Since fibrinogen molecule has a rather open structure and/or higher affinity to the hydrophobic surface, it will induce less viscous losses per adsorbed particle than the proteins that are rather rigid and/or have lower affinity to the surface. Thus, conformational change during the adsorption process may result in a change of the relation between f_0 and C. The adsorption of fibrinogen onto PPY films may have two different processes. Initially, a more rigid layer was formed, and then a looser layer came subsequently. A likely interpretation is that the newly incoming proteins attached in a different way resulted in a less rigid structure of the surface adsorption layer. And further discussion will be given below.

For studying the protein adsorption model, EQCIS was used to monitor the adsorption processes of both proteins. The results of Δf_0 and ΔC_s and other parameters of PQC resonance are shown in Figs. 7 and 8. Adding proteins in all cases led to abrupt decrease in the PQC frequency, showing that the adsorption of BSA and fibrinogen onto the surfaces took place. The change of R and $\Delta f_{G1/2}$ are also shown in Figs. 7 and 8, respectively. R_1 and $\Delta f_{G1/2}$ increased when the stock protein solution was added into the buffer solution, but then the change became slower with time. Changes in R_1 and $\Delta f_{G1/2}$ reflected the viscosity change of the solution or the film deposited on the electrode. But the absolute value of $\Delta f_0/\Delta R_{1L}$ was much larger than 10.14 Hz Ω^{-1}, suggested that the mass effect predominated in the protein adsorption process and the effect of viscosity could be neglected. Therefore, Δf_0 could be taken as an approximate measure of the mass of protein adsorbed on the tested surfaces via the Sauerbrey equation and the curve of Δf_0 versus time reflected the adsorption kinetics of the protein. The larger Δf_0, the more protein molecules adsorbed onto the electrode surface.

In addition, the interfacial capacitance, C_s, could reflect the protein adsorption behavior on the interface. The C_s data given here were obtained from the EIS based on serial R_s-C_s equivalent circuit in the absence of electrical active species [51]. And it also reveals the adsorption kinetics of the protein because protein adsorption onto the surface can cause change in interfacial capacitance through hindering or permitting the polar water in or near the electrode [37]. It is well known that the hydrophobic surface would somewhat hamper the accumulation of polar water molecule which has large permittivity near the electrode surface. The reason would be that the chance of water molecules or electrolyte ions entering into the electrical double-layer decreased when protein adsorbed onto the surface and led to an observable decrease in interfacial capacitance. The ΔC_s in Figs. 7 and 8 suggest that the adsorption of protein can change the interface capacitance notably.

It was found that the time-dependent response of Δf_0 and ΔC_s during protein adsorption process could be well simulated by the following experiential equation [17]:

$$Y_{(t)} = a_0 + a_1 e^{(-t/t_1)} + a_2 e^{(-t/t_2)} \tag{9}$$

where $Y_{(t)}$ can be either frequency response or interface capacity response, a_0, a_1, a_2, t_1 and t_2 are estimated parameters and t is the adsorption time. The parameter a_0 is the total frequency or interfacial capacitance shift when the adsorption time is long enough. These two exponentials suggest that two different kinetic steps are incorporated into the process of protein adsorption on the electrode surface. These two steps are the adsorption of protein molecules and the rearrangement

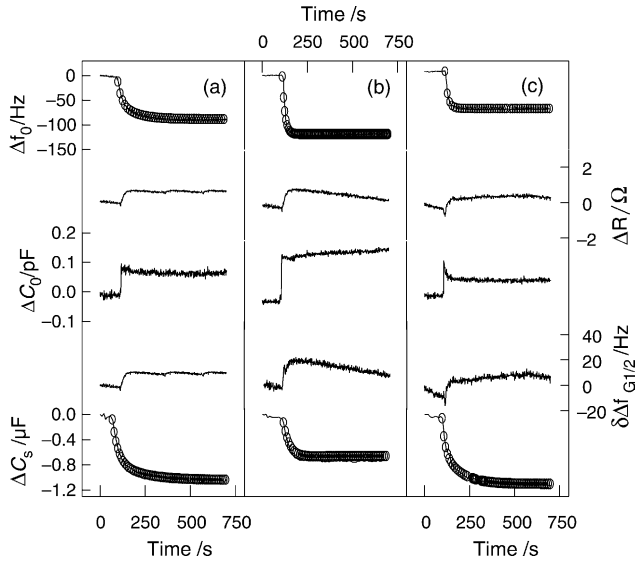

Fig. 7. The adsorption of BSA on the three obtained modified electrodes in 0.1 mol L^{-1} PBS (pH=7.0) under magnetic stirring (a) PPY/DBS-I, (b) PPY/DBS-II, (c) PPY/DBS-III. The final concentration of BSA was 20 μmol L^{-1}. EIS measurements: 3000 Hz and 10 mV rms, open circuit potential.

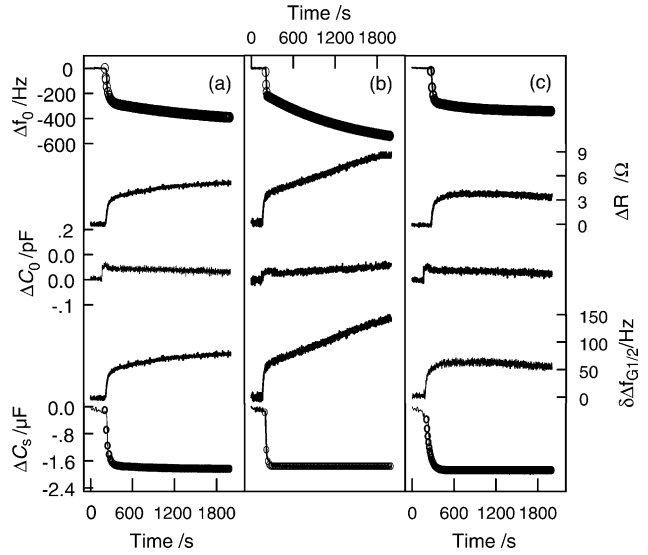

Fig. 8. The adsorption of fibrinogen on the three composite modified electrodes in 0.1 mol L^{-1} PBS (pH=7.0) under magnetic stirring (a) PPY/DBS-I, (b) PPY/DBS-II, and (c) PPY/DBS-III. The final concentration of fibrinogen is 4 μmol L^{-1}. EIS measurements: 3000 Hz and 10 mV rms, open circuit potential.

Table 3
Parameters obtained by fitting the responses of Δf_0 and ΔC_s given in Figs. 7 and 8 to Eq. (10)

PPY/DBS (C_{SDBS}) (mmol L^{-1})		a_0	a_1	a_2	t_1	t_2	q_r
BSA adsorption							
0.6	Δf_0 (Hz)	−90.0	6251.5	104.2	20.2	93.0	3.89×10^{-4}
	ΔC_s (μF)	−1.05	6.2	0.5	30.7	143.3	2.98×10^{-4}
1.2	Δf_0 /Hz	−120.3	182846.9	183749.3	14.1	14.2	9.24×10^{-4}
	ΔC_s (μF)	−0.67	−19.8	33.5	48.7	44.2	1.03×10^{-3}
2.0	Δf_0 (Hz)	−72.8	4613.8	8832783.1	23.4	9.5	4.98×10^{-4}
	ΔC_s (μF)	−1.1	387.7	1.7	14.9	91.1	2.16×10^{-3}
Fibrinogen adsorption							
0.6	Δf_0 (Hz)	−461.9	62138.3	211.2	38.7	1664.5	3.75×10^{-3}
	ΔC_s (μF)	−1.86	909.0	0.2	33.9	548.9	1.1×10^{-3}
1.2	Δf_0 (Hz)	−563.3	590.1	23.8	569.6	0.01	9.10×10^{-4}
	ΔC_s (μF)	−1.78	236157.3	5594.4	16.9	17.6	5.7×10^{-3}
2.0	Δf_0 (Hz)	352.0	291.5	180.9	307.2	309.3	7.2×10^{-4}
	ΔC_s (μF)	−1.98	910.8	0.18	33.9	582.9	3.87×10^{-3}

a_0, a_1, a_2, t_1 and t_2 are estimated parameters and a_0 is the total frequency or interfacial capacitance shift at infinite long time.

of the adsorbed protein molecules on the electrode surface, respectively. The Δf_0 and ΔC_s responses obtained were fitted using a non-linear fitting program embedded in Sigmaplot® Scientific Graphing Software Version 2.0. The relative sum of the residual squares is defined as:

$$q_r = \frac{q}{\sum_1^N r_{exp}^2} = \frac{\sum_1^N (r_{fit} - r_{exp})^2}{\sum_1^N r_{exp}^2} \quad (10)$$

where r_{fit} and r_{exp} denote the fitted and experimentally obtained response value of frequency or interfacial capacitance, respectively, and N is the number of the response signal points. The Δf_0 and ΔC_s of both proteins during the adsorption process were fitted with Eq. (9) and the results are listed in Table 3 and plotted as circles in Figs. 7 and 8. As mentioned above, a_0 is the total frequency or interfacial capacitance response at $t \to \infty$. Therefore, it could be inferred from Table 3 that the amounts of proteins adsorbed onto these three surfaces were different and needed different time to achieve their equilibriums, respectively. Much greater values of $\Delta f_{0,max}$ and $\Delta C_s(a_0)$ are obtained in the case of fibrinogen adsorption onto the three modified surfaces as compared to BSA adsorption (Table 3).

From the fitted results of $\Delta f_{0,max}(a_0)$ values, the amount of adsorbed proteins can be calculated based on the Sauerbrey equation (Eq. (1)), giving values of 0.46, 0.65 and 0.37 μg cm^{-2} for BSA and 2.51, 3.06 and 1.91 μg cm^{-2} for fibrinogen adsorption onto PPY/DBS-I, PPY/DBS-II and PPY/DBS-III surfaces, respectively. It is known that protein molecules adsorb on solid surface by 'side-on' or 'end-on' orientation with minor or major axes perpendicular to the surface [52]. Comparing the experimental data with the theoretical amount for the adsorption of BSA and fibrinogen [53], we suggested that BSA adsorption showed 'side on' adsorption model accompanied with 'end on' model on these three surfaces and mono-layered structures were formed. As for fibrinogen adsorbed on the three films, the 'end on' adsorption model prevailed and multi-layered structures were formed. This result can explain why the frequency constantly decreased even after 2000 s for fibrinogen adsorption while the frequency reached platform after 800 s for BSA adsorption during their saturated adsorption processes. Dupont-Gillain et al. obtained net-like structure of collagen adsorbed on poly(methyl methacrylate) with slow drying procedure [54]. And we suggested that network pattern of fibrinogen adsorption might be formed during fibrinogen adsorption process which caused by the properties of the mixed PPY/DBS film modified surface and the interplay between fibrinogen-film interaction and fibrinogen–fibrinogen interaction due to the change of the interaction speed.

4. Conclusions

Combined measurements of piezoelectric quartz crystal impedance (PQCI) and electrochemical impedance spectrum (EIS) were reported to monitor in situ adsorption of two model proteins (BSA and fibrinogen) on the hydrophilicity-controllable sodium dodecyl benzene sulfonate (SDBS)-doped polypyrrole (PPY) surfaces. These hydrophilicity controllable surfaces were easily obtained from electropolymerization of pyrrole in the presence of different concentrations of SDBS and three of these surfaces: PPY/DBS-I, PPY/DBS-II and PPY/DBS-III were chosen for further study of protein adsorption process. PPY/DBS-II obtained from electropolymerization of pyrrole solution containing 1.2 mmol L^{-1} SDBS, exhibited the greatest hydrophobicity as suggested by contact angle measurements. Using EQCIS, the kinetics and mechanisms of both proteins adsorption were investigated through studying the saturated adsorption behavior of both proteins on the three tested surfaces. Comparing the frequency and interfacial capacitance before and after the protein adsorption, we concluded that the adsorption models of the two proteins were different. BSA adsorbed on the three surfaces with 'end on' adsorption model accompanied with 'side on' model and monolayer was formed. And fibrinogen

adsorbed on the surfaces chiefly with 'end on' model and formed multi-layer structures. This work reveals that the surface hydrophilicity and/or hydrophobicity of polymer-modified electrodes could be adjusted by doping surfactants into the polymer film during the electropolymerization process. The adsorption capacity of polymer-modified electrode surface to protein and adsorption behavior of the protein is adjustable. Therefore, surfactant doped polymer film-modified electrodes would certainly find their extensive practical usage in biosensor and bio-analysis in future.

Acknowledgements

This work was supported by the National Natural Science Foundation of China (20335020), the Basic Research Special Program of the Ministry of Science and Technology of China (2003CCC00700), and the Foundation of the Ministry of Education (MOE) of China. (jiaorensi [2000] 26, jiaojisi [2000] 65).

References

[1] Andrade JD. Surface and interfacial aspects of biomedical polymers, vols.1 and 2. New York: Plenum Press; 1986.
[2] Brash JL, Horbett TA. Proteins at interfaces. ACS symposium series 343. Washington, DC: American Chemical Society; 1987.
[3] Norde W. Adv Colloid Interface Sci 1986;25:267–72.
[4] Ratner BD, Hoffman AS, Schoen FJ, Lemons JE, editors. Biomaterials science: an introduction to materials in medicine. San Diego: Academic Press; 1996.
[5] Horbett TA. Surfactant Sci Ser 2003;110:393–413.
[6] Jahangir AR, McClung WG, Cornelius RM, McCloskey CB, Brash JL, Santerre JP. Biomed Mater Res 2002;60:135–47.
[7] Shen M, Martinson L, Wagner MS, Castner DG, Ratner BD, Horbett TA. J Biomater Sci, Polym Ed 2002;13:367–90.
[8] Ostuni E, Grzybowski BA, Mrksich M, Roberts CS, Whitesides GM. Langmuir 2003;19:1861–72.
[9] Lu DR, Park K. J Biomater Sci, Polym Ed 1990;1:243–60.
[10] Noinville V, Vidalmadjar C, Sebille B. J Phys Chem 1995;99:1516–22.
[11] Chen S, Liu L, Zhou J, Jiang S. Langmuir 2003;19:2859–64.
[12] Caruso F, Furlong DN, Ariga K, Ichinose I, Kunitake T. Langmuir 1998; 14:4559–65.
[13] Ariga K, Lvov Y, Kunitake T. J Am Chem Soc 1997;119:2224–31.
[14] Zhao HP, Feng XQ, Yu SW, Cui WZ, Zou FZ. Polymer 2005;46: 9192–201.
[15] Delano WL, Ultsch MH, Vos AM, Wells JA. Science 2000;28:71279.
[16] Yang M, Fung FL, Thomson M. Anal Chem 1993;65:3713–6.
[17] Bernabeu P, Tamisiter L, Cesare AD, Caprani A. Electrochim Acta 1988; 33:1129–36.
[18] Vanysek P, Reid JD, Craven MA, Buck RP. J Electrochem Soc 1984;131: 1788–91.
[19] Buttry DA, Bard AJ, editors. Electroanalytical chemistry, vol. 17. New York: Marcel Dekker; 1991.
[20] Muramatsu H, Tamiya E, Karube I. Anal Chem 1988;60:2142–6.
[21] Martin SJ, Granstaff VE, Frye GC. Anal Chem 1991;63:2272–81.
[22] Xie QJ, Xiang CH, Zhang YY, Yuan Y, Liu MM, Nie LH, et al. Anal Chem Acta 2002;464:65–77.
[23] Yamaguchi S, Shimomura T, Tatsuma T, Oyama N. Anal Chem 1993;65: 1925–7.
[24] Xie QJ, Wang J, Zhou AH, Zhang YY, Liu HW, Xu ZN, et al. Anal Chem 1999;71:46–53.
[25] Sato T, Serizawa T, Okahata Y. Biochim Biophys Acta 1996;1285: 14–20.
[26] Cao CN. Electrochim Acta 1990;35:831–6.
[27] Zhu H, Snyder M. Curr Opin Chem Biol 2001;5(1):40–5.
[28] Gerard M, Chaubey A, Malhotra BD. Biosens Bioelectron 2002;17: 345–59.
[29] Fernandes KF, Lima CS, Pinho H, Collins CH. Proc Biochem 2003;38: 1379–84.
[30] Kholodovych V, Smith JR, Knight D, Abramson S, Kohn J, Welsh WJ. Polymer 2004;45:7367–79.
[31] Smith JR, Kholodovych V, Knight D, Kohn J, Welsh WJ. Polymer 2005; 46:4296–306.
[32] Kita-Tokarczyk K, Grumelard J, Haefele T, Meier W. Polymer 2005;46: 3540–63.
[33] Zhang YY, Fung YS, Sun H, Zhu DR, Yao SZ. Sens Actuators, B 2005; 105:454–63.
[34] Wise DL, Winek GE, Trantolo DJ, Cooper TM, Gresser JD. Electrical and optical polymer systems. New York: Marcel Dekker, Inc.; 1998 p. 17.
[35] Rodriguez J, Grande HJ, Otero TF. In: Nalwa HS, editor. Handbook of organic conductive molecules and polymers. New York: Wiley; 1997. p. 415.
[36] Simonet J, Berthelot JR. Prog Solid State Chem 1991;21:1–48.
[37] Sadik OA, Cheng MC. Talanta 2001;55:929–41.
[38] Lenz DM, Delamar M, Ferreira CA. J Electroanal Chem 2003;540:35–44.
[39] Lee H, Yang H, Kwak J. Electrochem Commun 2002;4:128–33.
[40] Li YL, Liu ML, Xiang CH, Xie QJ, Yao SZ. Thin Solid Films; in Press.
[41] Gordon JS, Jhonson DC. J Electroanal Chem 1994;365:267–74.
[42] Krivan E, Visy C, Kankare J. J Phys Chem B 2003;107(6):1302–8.
[43] Tian B, Zerbi G. J Chem Phys 1990;92(6):3886–91.
[44] Standard infrared grating spectra, vols. 21–22, Spectrum 21112 K, Philadelphia, PA: Sadtler Research Laboratories Inc.; 1971.
[45] Shen R, Zheng LX, Gao HW. Chin J Process Eng 2003;3:328–34.
[46] Anthony JP, Wang ZY, Rudin A. J Colloid Interface Sci 1995;173: 376–87.
[47] Yang XH, Xie QJ, Yao SZ. Synth Met 2004;143:119–28.
[48] Collepardi M. Cem Concr Compos 1998;20:103–12.
[49] Parfitt GD, Rochester CH, editors. Adsorption from solution at solid/liquid interfaces. London: Academic Press; 1983.
[50] Li HT, Jiao YC, Xu MC, Shi ZQ, He BL. Polymer 2004;45:181–8.
[51] Bard AJ, Faulkner LR. Electrochemical methods: fundamentals and applications. New York: Wiley; 1980.
[52] Tang Q, Xu CH, Shi SQ, Zhou LM. Synth Met 2004;147:247–52.
[53] Baszkin A, Lyman DJ. J Biomed Mater Res 1980;14:393–430.
[54] Dupont-Gillain CC, Nysten B, Rouxhet PG. Polym Int 1999;48:271–6.